ADVANCED MATERIALS
www.advmat.de
Materials Views
www.MaterialsViews.com

COMMUNICATION

A Novel Photoelectric Conversion Yarn by Integrating Photomechanical Actuation and the Electrostatic Effect

Xinghai Yu, Jian Pan, Jue Deng, Jun Zhou, Xuemei Sun, and Huisheng Peng**

Photoelectric conversion plays an important role in various electronics for detection, information, and energy supply. It is generally realized by solar cells that directly transform light into electricity.[1–5] However, their photovoltaic performances strongly depend on the weather condition, e.g., being less effective at a cloudy or rainy day. It is also difficult to control them remotely for a tunable photoelectric conversion, which may limit their practical applications in a variety of fields such as microelectronics. Therefore, a lot of efforts have been attempted to find the other strategies to convert the light energy to electricity with easy operation and high performance,[6–9] but it remains unavailable yet.

The rapid advancement on the multifunctional integration at electronics may provide a new and general platform to solve the above problem. Besides the direct photoelectric conversion by the solar cell, it reminds us whether the photoelectric conversion can be also realized indirectly by a series of functional parts that are integrated into one device. For instance, light energy can be first changed to the other forms of energy such as mechanical energy, followed by the further conversion to electricity.

On the one hand, a variety of materials such as polymers is studied to mechanically actuate upon the light irradiation, and this photomechanical actuation is reversible under alternate irradiation of different wavelengths of lights or periodical irradiation of the same light.[10–14] On the other hand, a material with the designed structure may generate electricity on the basis of piezoelectric, triboelectric or electrostatic effects under mechanical actuations.[15,16] Although the photomechanical actuation and the piezoelectric/triboelectric/electrostatic behavior are both extensively investigated, they have not been integrated to complete a series of energy transformations from light energy to mechanical energy and then to electrical energy, although it seems obvious and very promising to make such an integration. The difficulty lies in the selection of appropriate photoactive and electronic materials and the design of efficient structures and shapes.

Here, we have achieved such a novel photoelectric conversion device by effectively integrating the photomechanical actuation and electrostatic effect into a 1D yarn. The yarn-type photoelectric conversion device (YPCD) was composed of two functional electrodes (**Figure 1**a and Figure S1 and S2, Supporting Information). One electrode included an aligned carbon-nanotube (CNT) fiber that had been coated with poly(tetrafluoroethylene) (PTFE) to store charges, while the other electrode was made with a bilayer composite strip of aligned CNT sheet/paraffin wax/polyimide (PI) for photomechanical actuation. Under the periodical irradiation of visible light, the YPCD was repeatedly bent and released to change the distance between the composite strip and the fiber electrodes, which further changed the number of induced charges on them to generate potential differences. These YPCDs were flexible and foldable (Figure 1b,c), and they exhibited tunable output voltages with a high long-term stability, so they were promising for a broad spectrum of applications such as smart and flexible electronics with the requirement of remote control. This work also provides a new concept for photoelectric conversion other than solar cells.

The CNT fibers and sheets were dry-drawn from a spinnable CNT array that had been synthesized by chemical vapor deposition. The building CNTs were aligned in both fiber and sheet (Figure 1d,e), which provided them with flexibility and high electrical conductivity on the level of 10^2–10^3 S cm^{-1}. PTFE, as a polymeric electret, can retain electrostatic charges on surfaces for a long period.[17] PTFE nanoparticles with diameters of about 200 nm were dip-coated onto the CNT fiber to form a compact layer (Figure 1f,g). The composite fiber was polarized via plasma treatment to produce negative electrostatic charges on the PTFE surface.[18] The composite strip electrode was prepared by sequentially coating the molten paraffin wax and paving aligned CNT sheets on the PI film. The paraffin wax/CNT composite layer and PI film were compactly contacted with each other with the thickness of ≈20 and ≈10 µm, respectively (Figure 1h). The surface of the composite strip was smooth, with the paraffin wax uniformly filled in the voids of highly aligned CNTs (Figure 1i).

In a bilayer composite strip electrode, the aligned CNTs can absorb visible light to generate heat and efficiently transform the heat to the guest paraffin wax.[19] Because the thermal expansion coefficient of the paraffin wax is higher than that of PI film,[20] the bilayer composite strip was bent to the side of PI layer under the light. Furthermore, the aligned CNTs have a higher modulus in longitudinal direction than in transverse direction. This would exert a geometrical constraint to make the paraffin wax expand more perpendicularly to the aligned

X. Yu, J. Pan, J. Deng, Dr. X. Sun, Prof. H. Peng
State Key Laboratory of Molecular Engineering of Polymers
Collaborative Innovation Center of Polymers and Polymer Composite Materials
Department of Macromolecular Science and Laboratory of Advanced Materials
Fudan University
Shanghai 200438, China
E-mail: sunxm@fudan.edu.cn; penghs@fudan.edu.cn
Prof. J. Zhou
Wuhan National Laboratory for Optoelectronics and School of Optical and Electronic Information
Huazhong University of Science and Technology
Wuhan 430074, China

DOI: 10.1002/adma.201603206

© 2016 WILEY-VCH Verlag GmbH & Co. KGaA, Weinheim

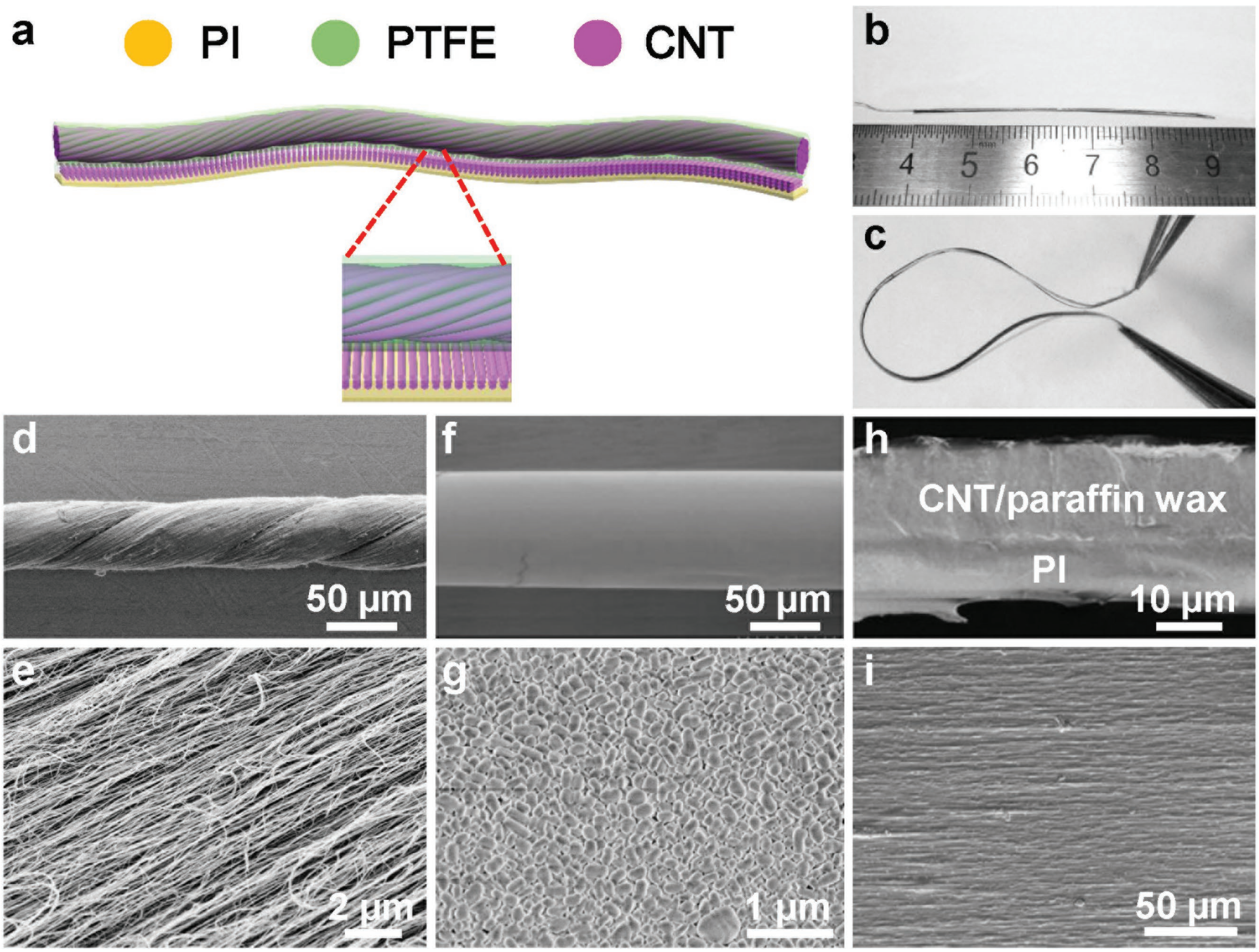

Figure 1. Schematic illustration and structure characterization of the YPCD. a) Schematic illustration. b,c) Photographs of the YPCD before and after bending, respectively. d,e) SEM images of an aligned CNT fiber at low and high magnifications, respectively. f,g) SEM images of a PTFE-coated CNT fiber at low and high magnifications, respectively. h,i) SEM images of the CNT/paraffin wax/polyimide composite strip in cross-sectional and side views, respectively.

CNTs (Figure S3, Supporting Information). Therefore, the bilayer composite strip exhibited bending deformation under the light, and could be recovered after removal of the light due to the volume change of the paraffin wax.[21] For a typical composite strip with a length of 3 cm, it was bent to a maximal displacement of 1.7 cm in ≈1.28 s under the light, and recovered in ≈2.00 s after turning off the light (Figure S4, Supporting Information). In addition, the alignment of CNTs also ensured the high reversibility and stability of photomechanical actuations.[21]

By assembling the composite strip with the PTFE-coated fiber, the resulting YPCD still exhibited bending deformation under the irradiation of visible light (**Figure 2**a). More specifically, when the CNT/paraffin wax composite layer was entirely irradiated by the visible light, the YPCD was bent to the side of PI layer within ≈2.05 s and generated a displacement of 1.4 cm for a 3 cm long strip; it was returned to the original state within ≈2.19 s after removing the light. The deformation had a longer response time and smaller displacement than the bare stripe electrode due to the constraint of the composite fiber electrode. Meanwhile, the distance between the two electrodes changed during bending under optical microscopy (Figure S5, Supporting Information). When the YPCD was bent under the light, the distance between the PTFE-coated CNT fiber and bilayer composite strip electrodes decreased gradually from ≈100 µm until contact, which was reversed after removal of the light. This reversible distance changes from reversible photomechanical actuation can be used to achieve the energy conversion based on the electrostatic effect.

The typical photoelectric conversion performance was studied by periodically turning on and off the light which was irradiated on the YPCD. Without the light irradiation, no obvious voltage signal was detected (Figure 2b). When the light was turned on, it bended to generate a positive voltage (Figure 2c); it was recovered to the original state and generated a negative voltage after turning off the light. For a typical YPCD with a length of 3 cm, the output voltage with a peak value of 70 mV was produced. With the light being turned on and off periodically, the YPCD was bent and released reversibly, thus generating the voltage signals at a specific frequency.

To illustrate the working principle, the YPCD was simplified into an equivalent circuit model (Figure 2d–f). Originally,

© 2016 WILEY-VCH Verlag GmbH & Co. KGaA, Weinheim

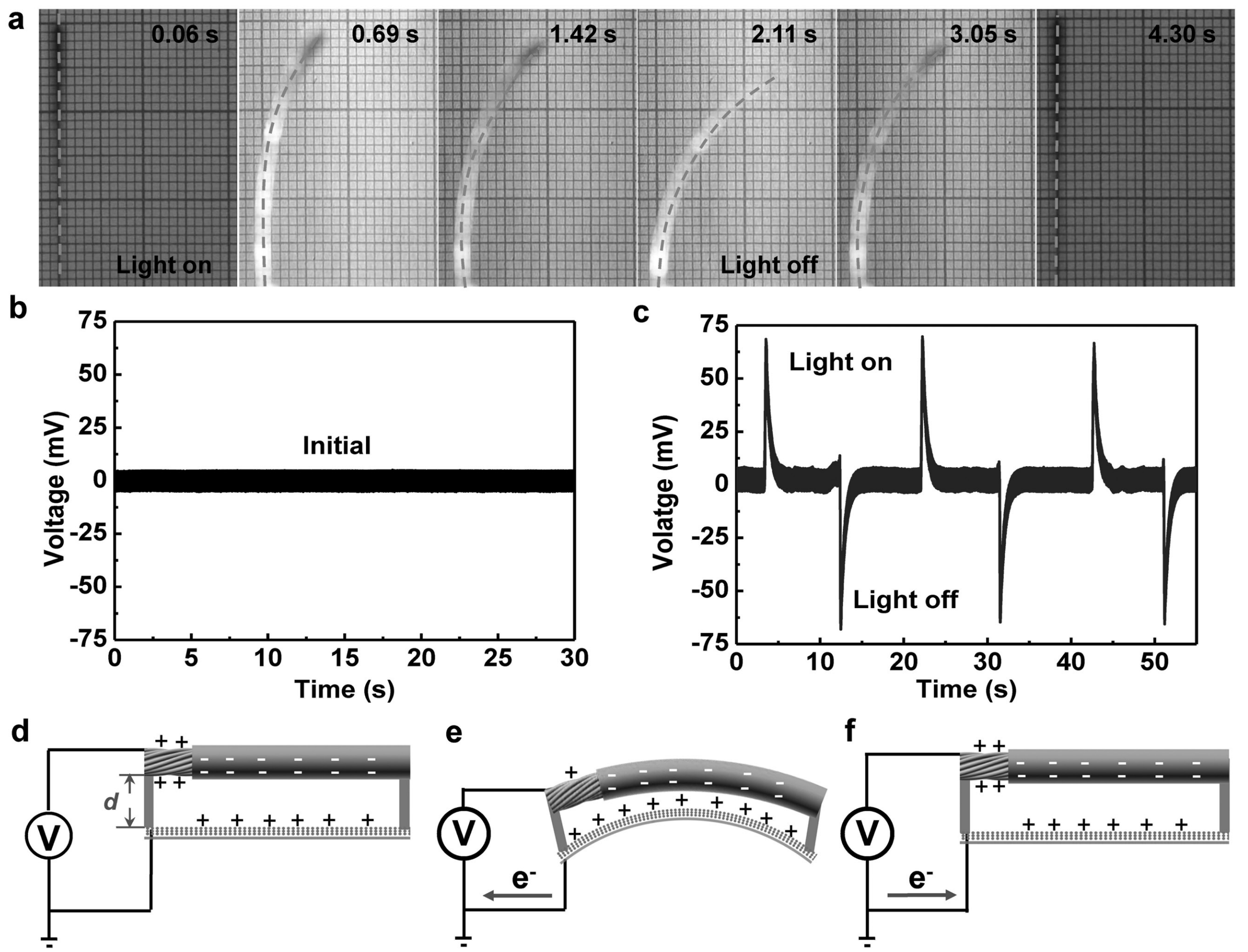

Figure 2. Working mechanism of the YPCD. a) Photographs of the YPCD (length of 3 cm, width of 0.2 cm) showing a reversible bending deformation in response to the visible light with an irradiated intensity of 27 mW cm^{-2}. b) The output signal at original state without the light irradiation. c) The output voltage with the light being periodically turned on and off. d–f) Schematic illustration of the charge distribution at the original state (d), under light irradiation (bending state) (e), and without light irradiation (after release) (f).

the PTFE layer was negatively charged by plasma polarization, while the CNT sheet was grounded. Due to the electrostatic effect, positive charges would be induced on the CNT fiber and sheet for the conservation of charges.[22,23] There was not any difference in electrical potential between the CNT fiber and sheet electrodes. When the YPCD was bent under the light, the distance between the PTFE coated CNT fiber and bilayer composite strip electrodes would decrease, and more positive charges were accumulated in the CNT sheet electrode because of the electrostatic induction. Therefore, an electrical potential difference was generated between the CNT fiber and sheet. Free electrons at the CNT sheet would flow to the CNT fiber to balance the potential difference and reached a new stable state after bending. When the YPCD was recovered to the original state after the light was turned off, the internal gap between PTFE coated CNT fiber and bilayer composite strip was increased to break the equilibrium. Therefore, the electrons flowed back from the CNT fiber to the CNT sheet through the external circuit, and an opposite electrical potential was thus produced. Therefore, an alternate output voltage had been observed, indicating that the YPCD was able to convert the light into electrical energy.

Specifically, taking one cycle in Figure 2c for demonstration (Figure S6, Supporting Information), when the light was turned on at 1.50 s, the YPCD was bent to the maximal displacement at 3.55 s and generated a maximal positive voltage of 70 mV due to the electrostatic induction along with the distance decrease of the two electrodes. After that, the bending was kept under the light, but the voltage decreased to the original value due to the flow of free electrons for balance. When the light was turned off at 10.32 s, the YPCD recovered to the flat form at 12.51 s. At the same time, it generated a negative voltage with the maximal value of 70 mV due to the increase of the internal gap between two electrodes. The voltage was then recovered again to the stable stage of original value because the electrons flowed back. The response time of the voltage generation was consistent with the bending deformation of the YPCD.

In order to confirm that the signal was generated by the YPCD rather than the measurement system, the switching polarity test was made to exclude the possible error from the

© 2016 WILEY-VCH Verlag GmbH & Co. KGaA, Weinheim

change in the system capacitor.[24] The YPCD can be considered as a variable-capacitance generator due to the stable charges in PTFE, and the change of the contact resistance might produce a disturbing signal under working. Such a signal could not change its sign when the positive and negative probes of voltage meter were exchanged. In contrast, for a YPCD with forward connection, the positive and negative voltage pulses corresponded to the rapid bending and recovering processes, respectively (Figure S7a, Supporting Information). However, the polarity of the output voltage signals was reversed but with similar values in the case of the exchanged connection under the same reversible photomechanical actuation process (Figure S7b, Supporting Information). Therefore, the measured signals were generated by the YPCD during the bending and releasing processes.

As the voltages were generated by the photomechanical actuation and the electrostatic effect, the frequency/irradiated intensity of the irradiation light and the content/polarization of PTFE were important factors to influence the output performance. **Figure 3**a shows the impact of the light frequency. For a given light with an irradiated intensity of 27 mW cm^{-2}, when the frequency of the light was increased from 0.2 to 0.6 Hz, the peak value of the output voltage was decreased. Under the light with the same frequency of 0.6 Hz, the peak value of the output voltage was increased from 50 to 150 mV with the increasing irradiated intensity of the light from 27 to 90 mW cm^{-2} (Figure 3b). This can be explained by the fact that the two factors decided the reversible bent displacement of the YPCD under the light. Higher irradiated intensity and lower frequency of the light would cause larger displacements, which thus led to higher peak output voltages. Similarly, the YPCD could generate different voltages in response to the light with different wavelength ranges (Figure S8, Supporting Information), which in turn could be used for photodetection. In other words, when an electrical signal was generated from the given YPCD, we can estimate the intensity, frequency or wavelength of the incident light.

As the PTFE was coated on the CNT fiber and polarized to store the charges, the content and polarization of PTFE were also important for the performance. For a given CNT fiber with

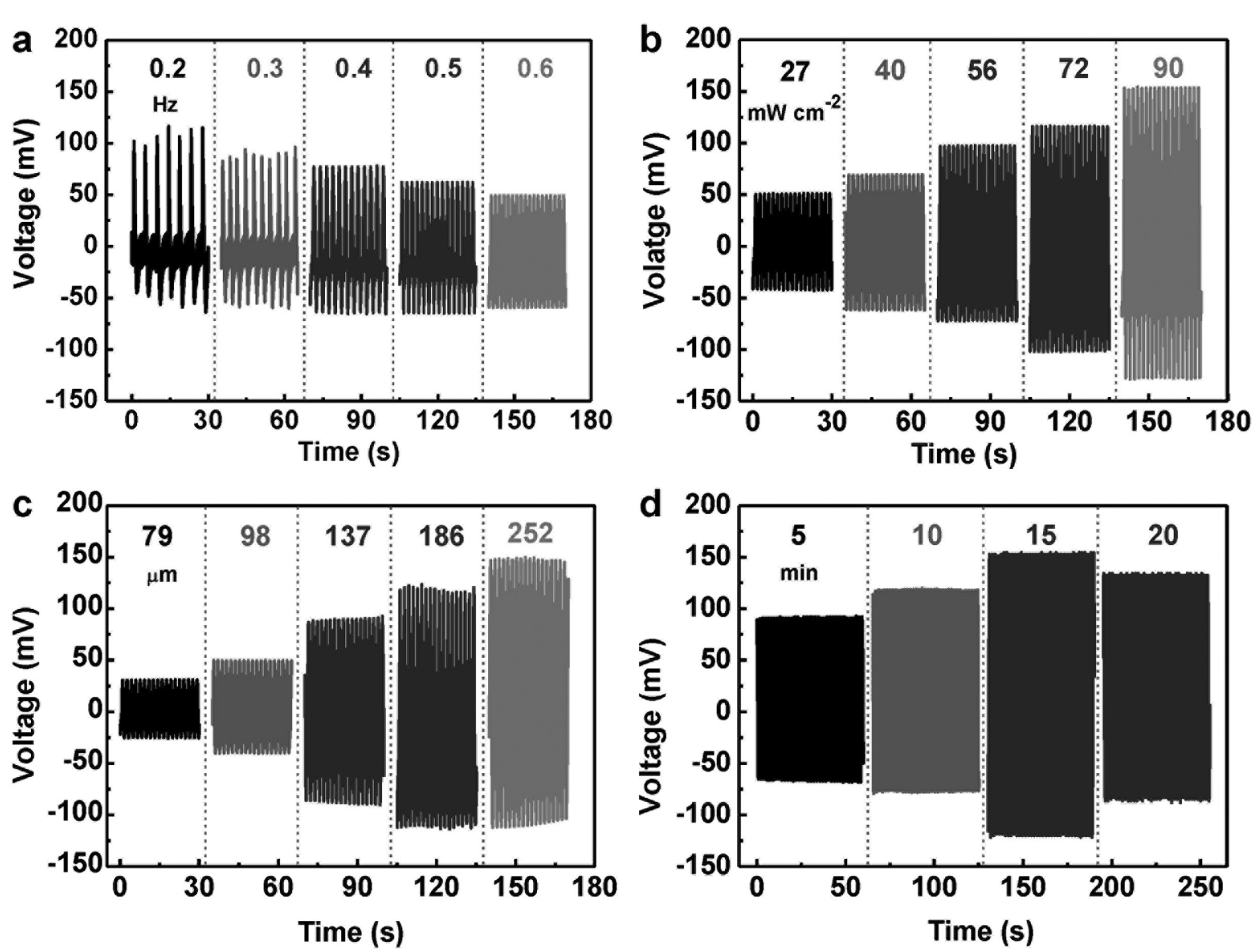

Figure 3. The output performance of the YPCD under different conditions. a) The output voltages under the irradiation light with increasing frequencies but the same irradiated intensity of 27 mW cm^{-2}. b) The output voltages under the irradiation light with increasing intensities but the same frequency of 0.6 Hz. c) The output voltages from the PTFE-coated CNT fibers with increasing diameters. d) The output voltages by polarization of PTFE for increasing periods.

© 2016 WILEY-VCH Verlag GmbH & Co. KGaA, Weinheim

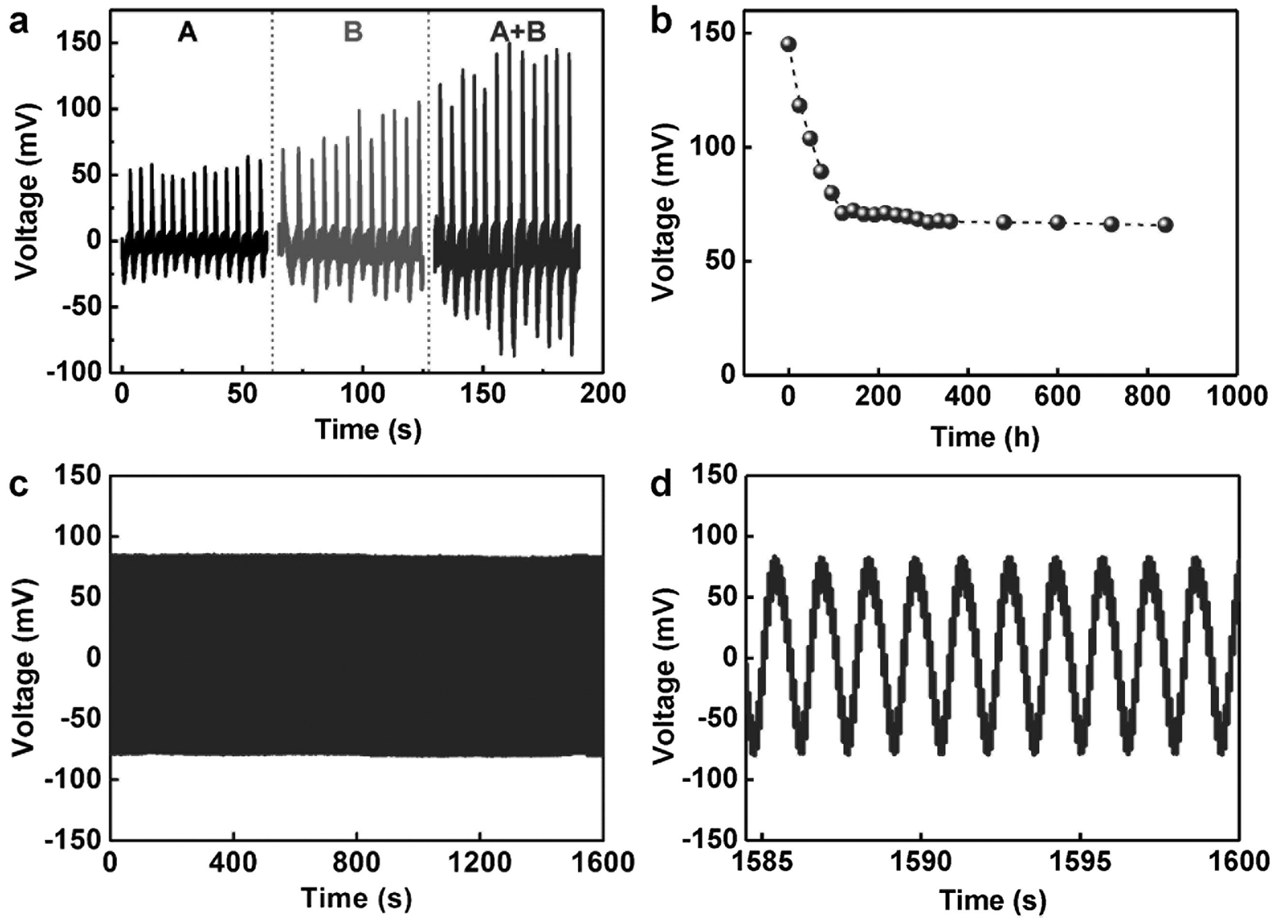

Figure 4. The integration and durability of the YPCD. a) The output voltages of two YPCDs (A and B) at separate state and parallel connection. b) The variation of the peak output voltage as a function of time. c) Continuous output performance of the YPCD for over 1000 cycles. d) The last ten cycles of (c).

the diameter of ≈54 µm, a series of PTFE-coated CNT fibers were prepared with the diameters in the range of 79–252 µm (Figure S9, Supporting Information) and polarized at the same conditions. The fabricated YPCDs showed increasing output voltages with the increasing diameters under the same condition (Figure 3c), as the surface area of the PTFE was improved to further increase the amount of negative charges at the surface during polarization.[22] Therefore, more positive charges would be induced on the CNT fiber and sheet due to the electrostatic effect, which finally enhanced the output voltages of the YPCD. Since the amount of the charges impregnated in PTFE by plasma polarization was essential to the output performance, the time of polarization was also investigated (Figure 3d). It was found that the output voltage displayed a significant increase with the increasing polarization time from 5 to 15 min; it was decreased with the further increase to 20 min in polarization time due to the surface damage of the PTFE layer under a longer polarization (Figure S10, Supporting Information), e.g., the PTFE may be peeled off from the CNT fiber during deformation.

The output voltages of the YPCDs can be also tuned. Two YPCDs (A and B) generated positive voltages when they were bent under light and produced negative voltages after releasing without the light. Under the light with an irradiation frequency of 0.2 Hz and an irradiated intensity of 27 mW cm^{-2}, the peak values of the positive output voltages were ≈50 mV for A and ≈100 mV for B, respectively, (**Figure 4**a). After being connected, the output voltages showed the same sign but with a superposed value of ≈150 mV under the same conditions. The result indicated that the output voltage from the connected YPCDs were enhanced compared to the single YPCD. The higher output performance with the increase in the number of YPCDs is attributed to the parallel connection (Figure S11, Supporting Information) which generated more induced charges.

Moreover, although the output voltage of a typical YPCD was decreased from ≈145 to ≈70 mV in the first 7 d, it could be then well maintained in the following 40 d (Figure 4b). As a typical polymer electret material, PTFE has been reported to be capable to implant negative charges by plasma polarization treatment. These implanted negative charges usually decay in two-stage.[25,26] In the first stage, they are compensated by relatively mobile intrinsic holes resulting in a comparatively steep decay nearly exponential, which is consistent with the first 7 d in this YPCD. After that, as the holes exhausted, the implanted negatives charge lied at a slow decay stage with the

 © 2016 WILEY-VCH Verlag GmbH & Co. KGaA, Weinheim

very long electret lifetime. This long-term performance was attributed to the high stability of PTFE to store the surface charges.[15] Further, a durability test was also carried out for over 1000 cycles of photomechanical actuation (Figure 4c). The output voltages remained almost unchanged due to the high reversibility of the photomechanical actuation of the composite strip.

The output power density of the YPCD was characterized by measuring the output voltage and current with an external load resistance. The YPCD (length of 3 cm, width of 0.2 cm) was connected with various load resistances from 5 kΩ to 100 MΩ and worked under the light with a frequency of 0.2 Hz. The peak output voltage increased from 25 to 150 mV with increasing load resistances, while the peak output current decreased from to 32 to 0 nA (Figure S12, Supporting Information). The instantaneous current and power values were 23.2 nA and 0.54 nW with an optimal external load resistance of 1 MΩ, respectively. The output current with the light being periodically turned on and off was recorded (Figure S13, Supporting Information). The average output power density of YPCD was calculated to be ≈0.38 nW cm^{-2} though an integration method (Figure S14, Supporting Information).[22]

In summary, a novel photoelectric conversion device in a yarn type was developed by integrating photomechanical actuation and electrostatic charge storage together. It could output a peak voltage of nearly 150 mV under the light irradiated. The photoelectric conversion performance was highly stable and durable, which is promising for long-term applications. This work also provides a new platform for converting light energy to electricity with high remote controllability.

Experimental Section

Preparation of the PTFE-Coated CNT Fiber: An aligned CNT fiber with a diameter of ≈54 µm was prepared from a spinnable CNT array that was synthesized by chemical vapor deposition.[27] An aqueous PTFE suspension (60%) was purchased from Aladdin and used as received. The PTFE was dip-coated onto the CNT fiber, followed by evaporation of solvent at room temperature. After being completely covered with PTFE, the composite fiber was annealed at 150 °C in an oven for 12 h in order to enhance the adhesion. Finally, the PTFE-coated CNT fiber was treated by plasma polarization (gas plasma generator, K-mate, China) with a service irradiated intensity of 75 W for 15 min, resulting in net negative electrostatic charges on its surface.

Preparation of the CNT/Paraffin Wax/Polyimide Composite Strip: The paraffin wax (from Sigma–Aldrich) was first melted at 80 °C and spin-coated onto a commercial polyimide film (*Kapton*, thickness of ≈10 µm) with a spinning speed of 1000 round per minute. Twenty layers of aligned CNT sheets (≈20 nm for each layer) were paved on the surface of paraffin wax. After reheating to 80 °C, the liquid paraffin wax was infiltrated into the aligned CNT sheet, followed by cooling to room temperature. The composite film was then cut into flexible strips with a length of 3 cm and width of 0.2 cm, and the CNTs were aligned along the width direction.

Fabrication of the Yarn-Type Photoelectric Conversion Device: The two ends of PTFE-coated CNT fiber electrode were fixed on the surface of CNT/paraffin wax/polyimide composite strip electrode by poly(vinyl alcohol) glue, leaving a gap between fiber and strip. Both the CNT fiber and sheet were bridged to one copper wire by silver paste for the connection with the external circuit. The YPCD with the length of 3 cm and width of 0.2 cm was typically studied in this work.

Supporting Information

Supporting Information is available from the Wiley Online Library or from the author.

Acknowledgements

This work was supported by NSFC (21225417, 51573027, 51403038), STCSM (15XD1500400, 15JC1490200), and the Program for Outstanding Young Scholars from Organization Department of the CPC Central Committee.

Received: June 18, 2016
Revised: July 27, 2016
Published online: October 10, 2016

[1] H. Zhou, Q. Chen, G. Li, S. Luo, T. Song, H. Duan, Z. Hong, J. You, Y. Liu, Y. Yang, *Science* **2014**, *345*, 542.
[2] M. Green, A. Ho-Baillie, H. Snaith, *Nat. Photonics* **2014**, *8*, 506.
[3] J. Chen, C. Cui, Y. Li, L. Zhou, Q. Ou, C. Li, Y. Li, J. Tang, *Adv. Mater.* **2015**, *27*, 1035.
[4] S. Pan, Z. Yang, P. Chen, X. Fang, G. Guan, Z. Zhang, J. Deng, H. Peng, *J. Phys. Chem. C* **2014**, *118*, 16419.
[5] H. Song, H. Tong, Z. Xie, L. Wang, F. Wang, *Chin. J. Polym. Sci.* **2013**, *31*, 1117.
[6] M. heldon, V. Jorik, A. Brown, P. Albert, H. Atwater, *Science* **2014**, *346*, 828.
[7] D. Francis, A. Amin, M. El-Khouly, N. Subbaiyan, M. Zandler, F. Shunichi, *J. Am. Chem. Soc.* **2012**, *134*, 654.
[8] Z. Meng, H. Bao, J. Wang, C. Jiang, M. Zhang, J. Zhai, L. Jiang, *Adv. Mater.* **2014**, *26*, 2329.
[9] A. McCormick, P. Bombelli, R. Bradley, R. Thorne, T. Wenzel, C. Howe, *Energy Environ. Sci.* **2015**, *8*, 1092.
[10] W. Wang, X. Sun, W. Wu, H. Peng, Y. Yu, *Angew. Chem., Int. Ed.* **2012**, *51*, 4644.
[11] X. Sun, W. Wang, L. Qiu, W. Guo, Y. Yu, H. Peng, *Angew. Chem., Int. Ed.* **2012**, *51*, 8520.
[12] Z. Jiang, M. Xu, F. Li, Y. Yu, *J. Am. Chem. Soc.* **2013**, *135*, 16446.
[13] S. Lin, Y. Wang, C. Cai, Y. Xing, J. Lin, T. Chen, X. He, *Nat. Nanotechnol.* **2013**, *24*, 10.
[14] L. Florea, K. Wagner, P. Wagner, G. Wallace, F. Benito-Lopez, D. Officer, D. Diamond, *Adv. Mater.* **2014**, *26*, 7339.
[15] S. Xu, Y. Qin, C. Xu, Y. Wei, R. Yang, Z. Wang, *Nat. Nanotechnol.* **2010**, *5*, 366.
[16] P. Yang, L. Lin, F. Yi, X. Li, K. Pradel, Y. Zi, C. Wu, J. He, Y. Zhang, Z. Wang, *Adv. Mater.* **2015**, *27*, 3817.
[17] J. Małecki, *Phys. Rev. B* **1999**, *59*, 9954.
[18] Q. Zhong, J. Zhong, B. Hu, Q. Hu, J. Zhou, Z. Wang, *Energy Environ. Sci.* **2013**, *6*, 1779.
[19] C. Li, Y. Liu, C. Lo, H. Jiang, *Soft Matter* **2011**, *7*, 7511.
[20] M. Lima, L. Na, J. Nica, F. Shaoli, O. Jiyoung, G. Spinks, M. Kozlov, C. Haines, S. Dongseok, F. Javad, *Science* **2012**, *338*, 928.
[21] J. Deng, J. Li, P. Chen, X. Fang, X. Sun, Y. Jiang, W. Weng, B. Wang, H. S. Peng, *J. Am. Chem. Soc.* **2016**, *138*, 225.
[22] J. Zhong, Y. Zhang, Q. Zhong, Q. Hu, B. Hu, Z. Wang, J. Zhou, *ACS Nano* **2014**, *8*, 6273.
[23] J. Zhong, Q. Zhong, Q. Hu, N. Wu, W. Li, B. Wang, B. Hu, J. Zhou, *Adv. Funct. Mater.* **2015**, *25*, 1798.
[24] R. Yang, Y. Qin, L. Dai, Z. Wang, *Nat. Nanotechnol.* **2009**, *4*, 34.
[25] G. Sessler, *J. Electrost.* **2001**, *51*, 137.
[26] J. Malecki, *Phys. Rev. B* **1999**, *59*, 9954.
[27] P. Chen, Y. Xu, S. He, X. Sun, W. Guo, Z. Zhang, L. Qiu, J. Li, D. Chen, H. Peng, *Adv. Mater.* **2015**, *27*, 1042.

© 2016 WILEY-VCH Verlag GmbH & Co. KGaA, Weinheim